Available online at www.sciencedirect.com
SCIENCE DIRECT®
International Journal of Thermal Sciences 42 (2003) 951–961
International Journal of Thermal Sciences
www.elsevier.com/locate/ijts

Non-contact photopyroelectric method applied to thermal and optical characterization of textiles. Four-flux modeling of a scattering sample ☆

Méthode photopyroélectrique sans contact appliquée à la caractérisation thermique et optique des textiles. Modélisation quatre-flux d'un échantillon diffusant

Angela Limare [a], Thierry Duvaut [b,*], Jean-François Henry [b], Christian Bissieux [b]

[a] *Institut français du textile et de l'habillement, 270, rue du Faubourg Croncels, 10042 Troyes cedex, France*
[b] *Laboratoire d'énergétique et d'optique, faculté des sciences, Moulin de la Housse BP 1039, 51687 Reims cedex 2, France*

Received 18 March 2002; accepted 18 January 2003

Abstract

The radiative transfer equation is solving considering the textile material equivalent to an absorbing and scattering slab and using a four-flux approach. Three macroscopic values of radiative parameters are accessible from a spectrophotometer used with an integrating sphere: the directional transmittance and the hemispherical reflectance and transmittance. The four-flux model for scattering with a linearly anisotropic phase function was used to identify the absorption and scattering parameters and the geometrical factor of the textile sample. For the nine investigated cotton samples, we showed that these parameters are related to the yarn, to structure and to water content. Then, the previously developed theoretical model for the photopyroelectric method in a noncontact configuration was modified for the case of a scattering sample using the same four-flux approach. The method was used for water content measurement and thermal parameters characterization of textile materials. Full description of the correlation analysis and inversion procedure and a synthesis of the results concerning the thermal parameters are given in a second article [Duvaut et al., Rev. Sci. Instrum. 73 (2002) 1299–1303].

Résumé

L'équation de transfert radiatif est résolue en considérant le matériau textile comme équivalent à un échantillon homogène absorbant et diffusant, et en utilisant un modèle 4 flux. Les valeurs macroscopiques de trois paramètres optiques sont mesurées à l'aide d'un spectrophotomètre muni d'une sphère intégrante : la transmittivité directionnelle, hémisphérique, et la réflectivité hémisphérique. Le modèle de diffusion à 4 flux avec une fonction de phase linéairement anisotropique est utilisé pour identifier les paramètres d'absorption et de diffusion, ainsi que le facteur géométrique de l'échantillon textile. Pour les neuf échantillons de coton testés, nous montrons que ces paramètres dépendent du titre du fil, de la structure du maillage et de la teneur en eau. Ainsi, le modèle théorique préalablement développé pour la méthode de photopyroélectricité dans une configuration sans contact, a été modifié pour permettre de traiter le cas des échantillons diffusants en utilisant une approche similaire quatre flux. La méthode est utilisée pour effectuer des mesures hygroscopiques et la caractérisation thermique de matériaux textiles. Dans le second article présenté simultanément avec celui-ci, nous effectuons l'analyse des corrélations entre les paramètres et de la procédure d'inversion, et nous présentons une synthèse des résultats concernant la mesure des paramètres thermiques de nos différents échantillons textiles.

Keywords: Photopyroelectric method; Four-flux modeling; Textile; Thermal parameters; Optical parameters

Mots-clés : Méthode photopyroélectrique ; Modélisation quatre-flux ; Textile ; Paramètres thermiques ; Paramètres optiques

☆ This work was financially supported by the Region Champagne Ardenne, France.
* Corresponding author.
E-mail addresses: angela.frandas@univ-reims.fr (A. Limare), thierry.duvaut@univ-reims.fr (T. Duvaut).

1290-0729/$ – see front matter
doi:10.1016/S1290-0729(03)00073-5

Nomenclature

a	phase function coefficient in the linearly anisotropic model		
C	volume specific heat	$J{\cdot}K^{-1}{\cdot}m^{-3}$	
c	specific heat	$J{\cdot}kg^{-1}{\cdot}K^{-1}$	
d_{air}	air gap thickness	m	
e	thermal effusivity	$W{\cdot}K^{-1}{\cdot}m^{-2}{\cdot}s^{1/2}$	
f	modulation frequency	Hz	
I_0	incident flux	$W{\cdot}m^{-2}$	
I^+, I^-	directional components of the flux	$W{\cdot}m^{-2}$	
K	absorption coefficient	m^{-1}	
L^+, L^-	isotropic components of the intensity on each half-space	$W{\cdot}m^{-2}{\cdot}sr^{-1}$	
L_λ	spectral intensity	$W{\cdot}m^{-2}{\cdot}sr^{-1}{\cdot}\mu m^{-1}$	
L°	blackbody intensity	$W{\cdot}m^{-2}{\cdot}sr^{-1}$	
l	sample thickness	m	
q_i	volume heat source of layer "i"	$W{\cdot}m^{-3}$	
p_λ	phase function		
S_{sample}	Heat source generated by the absorption into the sample	$W{\cdot}m^{-3}$	
S_{sensor}	Heat source generated by the absorption into the sensor	$W{\cdot}m^{-2}$	
T	Temperature	K	

Greek symbols

α_i	thermal diffusivity of layer "i"	$m^2{\cdot}s^{-1}$
β	extinction coefficient	m^{-1}
$\lambda_{th\,i}$	thermal conductivity of layer "i"	$W{\cdot}m^{-1}{\cdot}K^{-1}$
ρ_i	reflection coefficient of the surface "i"	
$\rho'^{\cap}$	directional hemispherical reflectance	
ρ_s	specular reflectivity at normal incidence	
ρ_p	specular reflectivity depending of the incident beam	
σ_i	complex heat diffusion coefficient of the layer "i"	m^{-1}
σ	scattering coefficient	m^{-1}
τ_i	transmission coefficient of the surface "i"	
τ'	directional transmittance	
$\tau'^{\cap}$	directional hemispherical transmittance	
Φ	net radiative flux	$W{\cdot}m^{-2}$

1. Introduction

Comfort of fabrics is mainly determined by their thermal insulation and water transport properties. This study enters into a more general concern of objective evaluation of comfort. Its purpose is the accumulation of experimental data concerning the thermophysical properties of textiles depending on the structure characteristics of the fabric, hydrophilic or hydrophobic character of constituent fibers, in order to obtain an expert system able to predict properties of virtual fabrics in different conditions of use.

The PhotoPyroElectric (PPE) method in noncontact configuration was chosen for the thermal parameters properties measurement due to its already proven efficiency [1]. The method allows the measurement of samples equilibrated at different water contents imposed by salt solutions [2]. Due to the capability of the pyroelectric sensors to respond to very small temperature variations, very low levels of excitation radiation could be used which prevented unwanted phenomena like desorption of water. Other photothermal methods have already been used for textile characterization like radiometry [3,4], needing generally higher excitation power.

The photothermal response depends on several properties of the sample: optical, thermophysical and geometrical. In the case of textile materials, "inhomogeneous" by definition, we normally expect to encounter difficulties when measuring their thermophysical properties. We can normally obtain only "average", "effective" values of the thermal parameters, nevertheless the only important in use conditions.

One method used up to now in textile industry for thermal parameters measurement is the one called Alambeta [5] where the sample is placed between two metal plates and pressure is applied during the measurement. Another method in use is the one called "the skin model" [6,7] where the thermal resistance is measured by the electrical power needed to keep a fabric at a constant temperature (35 °C). These methods can classify fabrics according to their insulation properties but the values are subject to large errors.

An important aspect of the interpretation of a photothermal signal is the modeling of the interaction of the incident radiation with the sample. The theoretical model of the noncontact PPE method did not take into account scattering, but only absorption and reflection.

One-dimensional radiative transfer in fibrous media has already been modeled using either multiflux approach or quadrature schemes, and radiative properties calculated on the basis of these models [8,9]. It has been shown that the four-flux approach gives sufficiently accurate results in experiments where collimated incident beams are used [9,10]. As for the phase function representation we have chosen only functions depending at most on one parameter. Three macroscopic values are accessible with a spectrophotometer used with an integrating sphere: the directional transmittance and the hemispherical reflectance and transmittance. Therefore, we could normally expect to identify a maximum number of three parameters characterizing the material: the absorption and the scattering coefficients and one parameter related to the anisotropy of scattering. A Levenberg–Marquart algorithm was used for parameter identification. We have showed that these parameters depend on the yarn, the stitch characteristics and the water content.

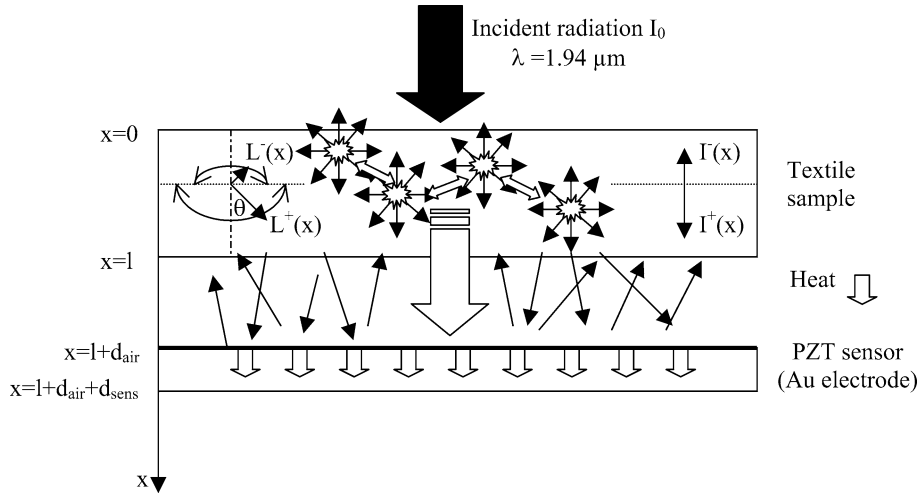

Fig. 1. Schematic of light and heat propagation into the textile sample/pyroelelectric sensor assembly.

The four-flux model is also compatible with the PPE experiment, the only difference being a modified boundary conditions. The heat sources in the sample and sensor have been calculated, then the PPE amplitude and phase signal have used to identify the thermal parameters of the sample.

A laboratory prototype has been validated for the purpose of measuring the thermal insulation properties. This prototype have been developed initially for the water content measurement in thin layers of biodegradable packaging films based on starch, the measurement of the profile of water in this material and the study of its migration dynamics [2,11].

2. PPE model

A schematic of an experimental cell that makes use of a pyroelectric sensor in a noncontact configuration is shown in Fig. 1. The sensor placed behind the sample is separated from the sample by a thin air gap. The front electrode of the sensor has a high reflection coefficient. The first step of the modelling is the description of light propagation within the structure. A temperature rise is produced upon absorption and the heat diffuses. The temperature field in the three-layer structure is calculated. The pyroelectric signal is given by the temperature increase in the sensor, averaged over the sensor's thickness.

The lateral dimensions of the layers involved are large enough to decrease the 2D effects. The lateral heat loss is well described by heat exchange coefficient "*h*" in a 1D model. The 1D modelling of a scattering sample using a four flux approach is presented in the Appendix. Once the optical behaviour of textile samples is mastered, we proceeded with the modelling of the thermal response of the pyroelectric sensor placed in the vicinity of the sample, when the sample is illuminated by a collimated beam.

2.1. Equation of radiative transfer using the four-flux approach

In order to calculate the flux at each point of the sample and into the sensor front electrode, the mathematical model developed in Appendix A holds true except for the boundary condition at $x = l$. The distance between the sample and the sensor being very small compared with the structure's diameter of overall specimen, we can consider that a specular reflection is present at the interface between the sample and the air gap. Eqs. (A.6) and (A.12) become:

$$I^+(0) = \tau_0 I_0 \quad \text{and} \quad I^-(l) = \rho_s I^+(l) \tag{1}$$

$$L^+(0) = 0 \quad \text{and} \quad L^-(l) = \rho_p L^+(l) \tag{2}$$

where ρ_s is the specular reflectivity at normal incidence and ρ_p is the specular reflectivity depending on the polarization of the incident beam. The reflectivity ρ_p, given by the Fresnel equation, depends on the angle of incidence, therefore Eq. (2) has to be integrated for all the angles θ.

2.2. The heat sources and the PPE signal

The heat source generated by the absorption of the incident radiation into the sample can be calculated at each point by the divergence of the optical flux at that point. For a one-dimensional geometry, and for the four-flux model, we obtain:

$$S_{\text{sample}}(x) = -\frac{\mathrm{d}\Phi}{\mathrm{d}x} = -\frac{\mathrm{d}I^+(x)}{\mathrm{d}x} + \frac{\mathrm{d}I^-(x)}{\mathrm{d}x} - \pi\frac{\mathrm{d}L^+(x)}{\mathrm{d}x} + \pi\frac{\mathrm{d}L^-(x)}{\mathrm{d}x} \tag{3}$$

Using the differential equations (A.4), the heat source can be expressed by the flux terms directly:

$$S_{\text{sample}}(x) = K\big[I^+(x) + I^-(x)\big] + 2\pi K\big[L^+(x) + L^-(x)\big] \tag{4}$$

where we can easily verify that the heat source is zero if the sample is not absorbing.

Another contribution to the PPE signal is given by the absorption by the sensor front electrode of the transmitted light:

$$S_{\text{sensor}} = (1-\rho_s)I^+(l) + \pi\left[1-\int \rho_p(\theta)\sin\theta\,\mathrm{d}\theta\right]L^+(l) \tag{5}$$

The two heat sources were introduced into the already existing model for calculating the PPE signal [2,16]. This model makes use of the Green function, the sample being considered thermally homogeneous. By applying the superposition principle, the resulting temperature field will be given by the sum of the two separate temperature fields.

If the excitation light is modulated, the heat sources and the subsequent temperature fields in each layer are also modulated sinusoidally:

$$S(x,t) = S(x)\exp(j\omega t) \quad \text{and} \quad T(x,t) = T(x)\exp(j\omega t) \tag{6}$$

Then, the heat diffusion equation for each layer "i" (sample = "1", air gap = "2" and sensor = "3") can be written as follows:

$$\frac{\mathrm{d}^2 T_i(x)}{\mathrm{d}x^2} - \frac{j\omega}{\alpha_i}\cdot T_i(x) = -\frac{q_i(x)}{\lambda_{\text{th}\,i}} \tag{7}$$

where α_i and $\lambda_{\text{th}\,i}$ are respectively the thermal diffusivity and the thermal conductivity of the layer "i". The solutions have to satisfy the boundary conditions: the continuities of the temperature and of the heat flux at each interface.

The convective and radiative transfer at the interfaces with air ($x = 0$, $x = l + d_{\text{air}} + d_{\text{sens}}$) are characterized by the heat exchange coefficient h. For the other interfaces the heat transfer is only by conduction.

Considering only the first heat source (Eq. (4)), the solution of Eq. (7) for the sample can be found by the convolution of the heat source and the Green function, that is the solution obtained for a plane heat source at $x = z$ into the sample:

$$G(x,z) = C_1\exp(-\sigma_1 x) + D_1\exp(\sigma_1 x) + \frac{1}{2\lambda_1\sigma_1}\exp\bigl(\sigma_1|x-z|\bigr) \tag{8}$$

where $\sigma_i = (1+j)(\pi f/\alpha_i)^{1/2}$ is the complex diffusion coefficient of the layer "i"; the reciprocal of its real part being the thermal diffusion length.

For the second heat source, generated into the sensor front electrode, the temperature field in each layer is calculated using Eq. (7) without volume sources ($q_i = 0$) and with a modified boundary condition: i.e., a supplementary heat flux (S_{sensor}) is appearing at the interface air gap/sensor.

Then, the PPE signal, proportional to the average temperature over the sensor thickness was calculated, taking also into account the electronic transfer function of the amplifying system.

2.3. Numerical simulation of the theoretical signal

The purpose of our work is to identify the thermal parameters of a sample, so we have to measure the other parameters in order to reduce the number of unknown parameters. The parameters that we can measure prior to the PPE experiment are the coefficients related to optical absorption and scattering and the sample's thickness. The uncertainties on these "assumed to be known" parameters introduce deterministic errors into the signal amplitude and phase, equivalent to a measurement error. We compare the amplitude and phase sensitivities calculated from the model with respect to variations of the "assumed to be known" parameters and the respective experimental errors. From this comparison we obtain the precision needed on these parameters, so that their influence on the parameters to identify should be negligible.

We proceed with numerical simulations of the theoretical amplitude and phase in order to estimate the weight of each parameter (optical, thermal and geometrical) playing a role in the model.

Knowing the absorption coefficient K, the scattering coefficient σ, and the phase function, we can estimate the amplitude and the phase of the PPE signal. In Fig. 2 we present the amplitude and the phase of the PPE signal calculated using the model shown previously and the following input parameters for the sample: optical absorption coefficient $K = 200\ \mathrm{m}^{-1}$, scattering coefficient: $\sigma = 5000\ \mathrm{m}^{-1}$, phase function parameter: $a = 1$, thermal conductivity $\lambda_{\text{th}} = 0.12\ \mathrm{W{\cdot}m^{-1}{\cdot}K^{-1}}$, volume specific heat $C = 3\times10^5\ \mathrm{J{\cdot}K^{-1}{\cdot}m^{-3}}$; thickness $l = 1$ mm, air gap thickness $d_{\text{air}} = 0.5$ mm. The thermal parameters of the sensor are: thermal conductivity $1.2\ \mathrm{W{\cdot}m^{-1}{\cdot}K^{-1}}$, volume specific heat $3.28\times10^6\ \mathrm{J{\cdot}K^{-1}{\cdot}m^{-3}}$ and thickness 0.2 mm, corresponding to the values of the PZT ceramic used in the PPE experiment.

The heat exchange coefficient value ($h = 18\ \mathrm{W{\cdot}m^{-2}{\cdot}K^{-1}}$) is apparently very large for a confined environment, but it includes also the effect of lateral heat diffusion due to limited dimensions of the sensor.

The PPE amplitude was normalized to the sensor amplitude obtained when illuminated alone, without a sample. At

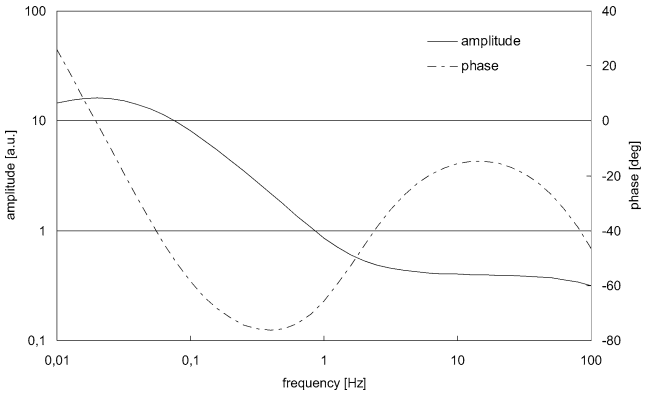

Fig. 2. Theoretical simulation for PPE amplitude and phase obtained with the model.

low frequencies the heat generated in the sample has a diffusion length large enough to reach the sensor. As the frequency increases, the heat wave into the sample is strongly attenuated, so the signal is given only by the transmitted light. The signal amplitude at high frequencies is given only by the heat source into the sensor electrode and is proportional to directional-hemispherical transmittance of the sample. Only the first heat source (S_{sample}, Eq. (4)) contains information on the thermal parameters of the sample, so the second one (S_{sensor}, Eq. (5)) should be reduced as much as possible. This is the reason why the front electrode was made highly reflecting (Au). The phase contains also information on the thermal parameters of the sample since the first heat wave is not only attenuated but also phase shifted. Actually, correlation analysis of the signal amplitude and phase shows that the phase is much more sensitive for thermal parameter evaluation, because the parameters are less correlated [17]. The information contained in the signal is limited, therefore the number of parameters that can be simultaneously identified is also restricted.

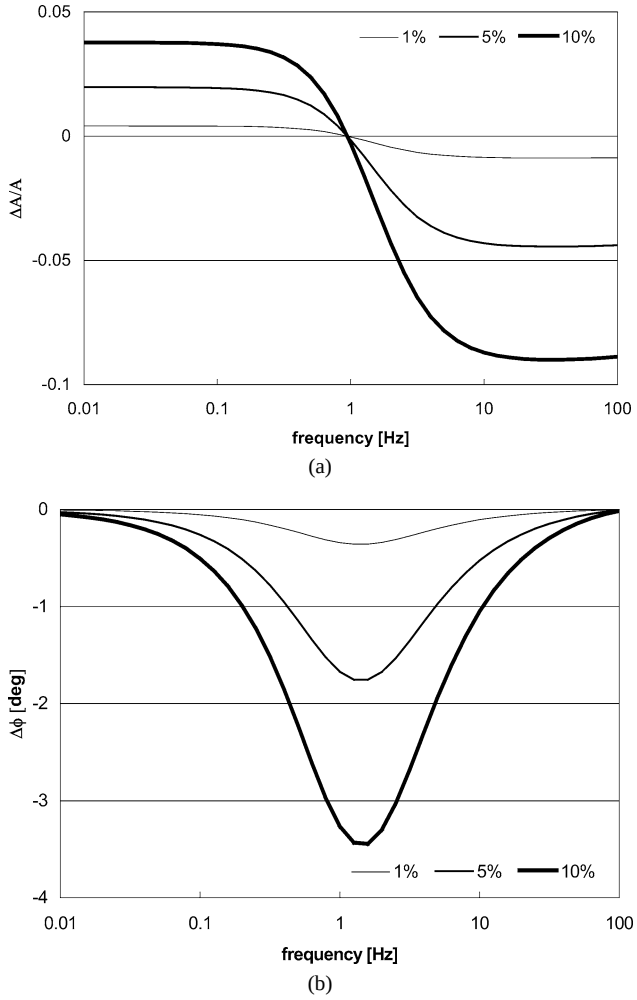

Fig. 3. Relative variations of amplitude (a) and phase (b) caused by 1%, 5% and 10% change in optical absorption coefficient of the sample.

The measurement error was at most 5% for the amplitude and 1 deg for the phase. We have calculated the relative variations of the amplitude and the phase of the PPE signal for some given variations of the "assumed to be known" parameters: 1%, 5% and 10%. Fig. 3 shows the theoretical results for the optical absorption coefficient variation. To avoid its influence on the results, the absorption coefficient has to be known with a precision better than 5%. This is effectively our case (see the experimental results) since the measurement uncertainty is about 4%.

Fig. 4 shows the theoretical results for the scattering coefficient variation. The uncertainty of this parameter should be slightly above 5%. We considered that a precision of about 7% as it is in our case was sufficient. The phase function parameter a has a smaller influence on the signal (results not shown), a absolute accuracy of 0.2 is thus roughly sufficient.

A very delicate parameter is the sample thickness. Fig. 5 shows that the uncertainty of this parameter should be about 3% or less. The thickness of a textile material depends on the pressure applied during the measurement. We applied the International Standard [18] that gives the value of the thickness at two applied pressures. The optical and then the

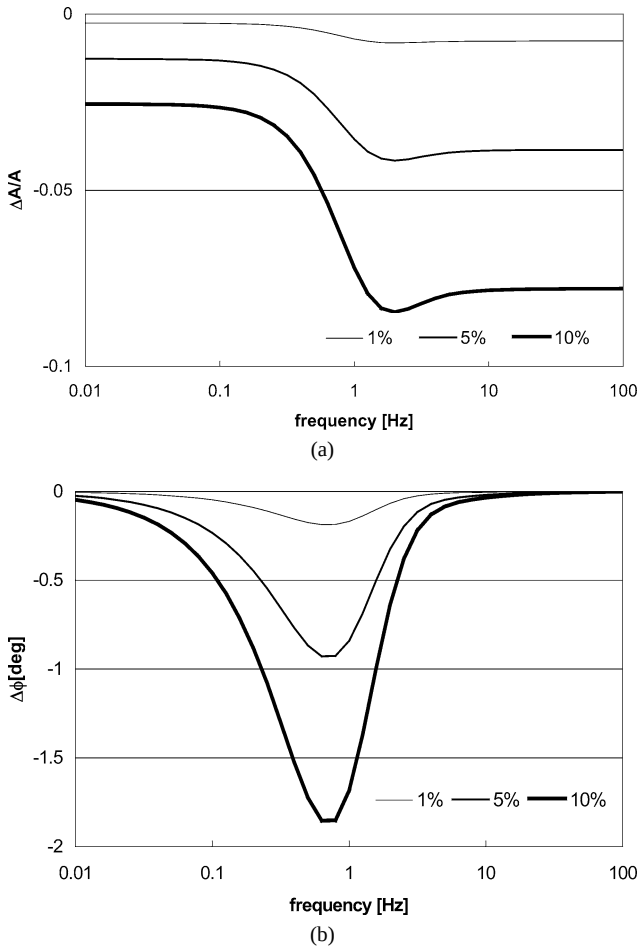

Fig. 4. Same as Fig. 3 for the scattering coefficient.

Table 1
The characteristics of jersey knitted samples measured at 20 °C and 65%RH. l_1 and l_2 are the values of sample thickness obtained by applying a pressure of 1 g·cm^{-2} and 10 g·cm^{-2}, respectively

Reference Sample	Yarn number/stitch	Absorbed stitch length [cm]	Mass per area [g·m^{-2}]	l_1(1 g·cm^{-2}) [mm]	l_2(10 g·cm^{-2}) [mm]
C21	28/1 *2	54	364	1.66	1.39
C22	28/1 *2	60	332	1.79	1.50
C23	28/1 *2	66	297	1.87	1.58
C41	40/1	29.7	200	1.13	0.80
C42	40/1	33	176	1.13	0.82
C43	40/1	36.3	162	1.10	0.82
C51	50/1	26.1	182	0.98	0.73
C52	50/1	29	171	1.07	0.80
C53	50/1	31.9	157	1.07	0.81

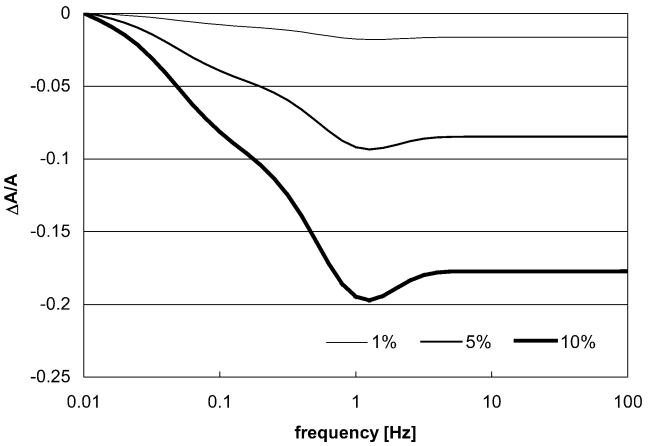

(a)

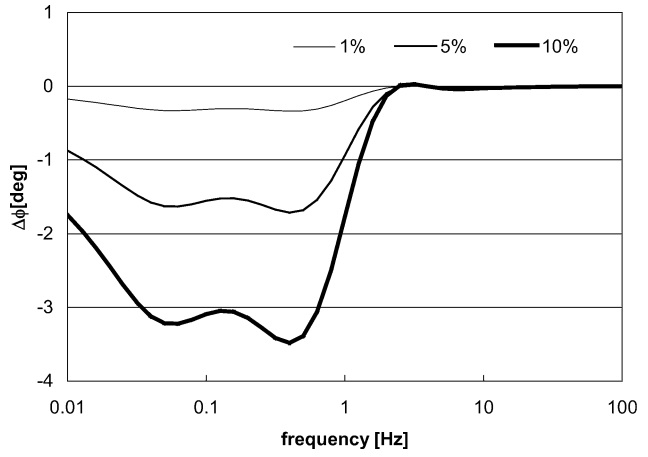

(b)

Fig. 5. Same as Fig. 3 for the thickness of the sample.

thermal parameters were identified using the two values of thickness.

3. Experimental results

Nine samples were chosen among some thirty other samples that we defined by changing only one parameter while the others were kept constant. The parameters that could change are the type of knitting, the yarn number N_e,[1] the absorbed stitch length[2] and the composition. This series of samples was defined and investigated in order to fill in a data base of experimental values for the thermophysical parameters, for the purpose of creating an expert system.

The results presented here concern only jersey knitted cotton samples, having three values of yarn number and for each type of yarn number three values of absorbed stitch length (see Table 1). The thickness for each knitted sample was measured at two pressure values 1 g·cm^{-2} and 10 g·cm^{-2} respectively (International Standard [18]). Samples C21, C22, C23 have 2 yarns per stitch, each of them having a yarn number of 28/1. The rest of the samples have 1 yarn per stitch.

3.1. Optical parameters

The directional-hemispherical radiative parameters were measured using a two-beam spectrophotometer (Lambda 9 Perkin–Elmer) equipped with an integrating sphere of 60 mm diameter. Three macroscopic values are accessible experimentally: τ', $\tau'^{\cap}$ and $\rho'^{\cap}$. These values are subject to errors due to the reduced dimensions of the integrating sphere. Therefore they were corrected by using Spectralon standard scattering samples and certified reflectance standards from Labsphere.

Since the maximum number of parameters that can be obtained experimentally is three, we have chosen for phase function representation only functions depending on one parameter at most. For each type of phase function defined in Section 1.3, the optical parameters were identified using a least-square minimization program based on a Levenberg–Marquart algorithm [14,15]. The best results were obtained with the LAS phase function (A17). The isotropic phase function is not adapted for the modeling of the radiation

[1] Yarn Number = the length in km of 1 kg of yarn. The larger this value, the finer the yarn.

[2] Absorbed Stitch Length = the length in cm of 100 stitches. The smaller this value the tighter the knitted.

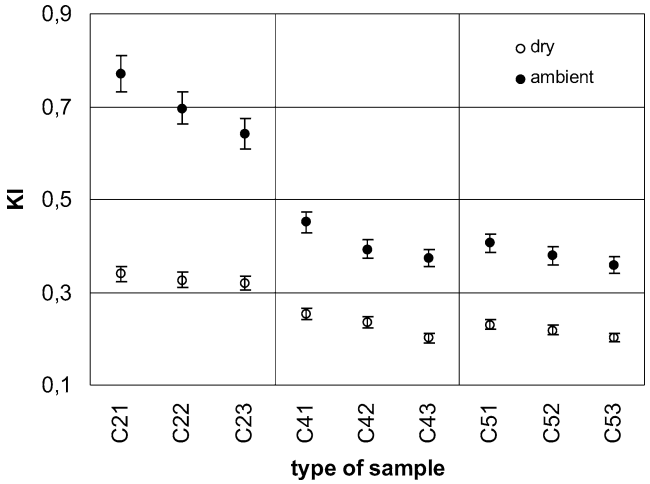

Fig. 6. Experimental values of the optical thickness Kl for dry and ambient cotton samples.

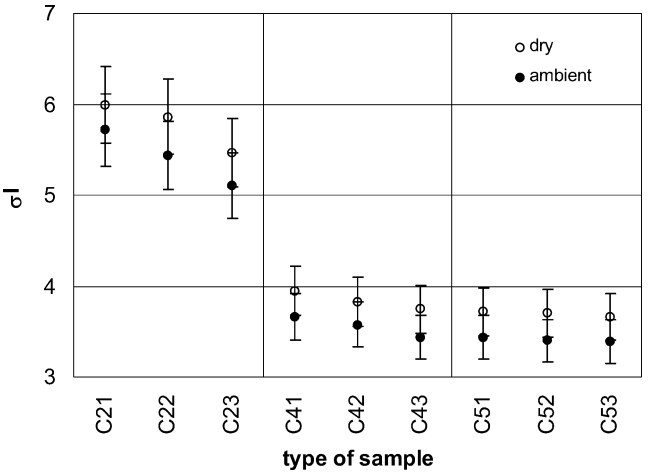

Fig. 7. Same as Fig. 6 for the scattering thickness σl.

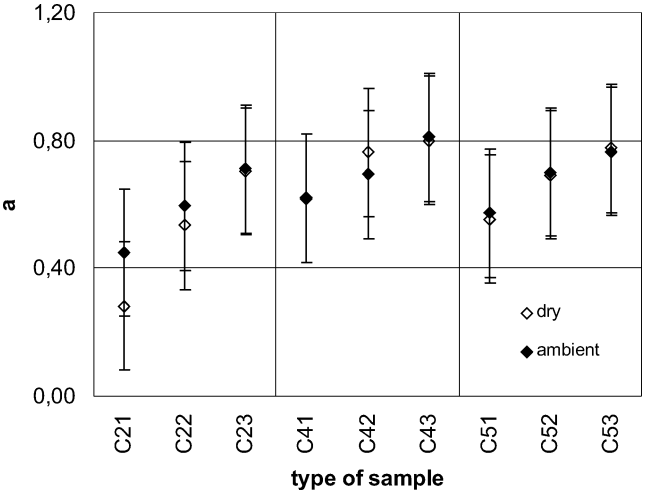

Fig. 8. Experimental values of the phase function parameter a for the dry and ambient cotton samples.

propagation into textiles because the numerical fit did not converge. The Henyey–Greenstein function depends on one parameter but gave numerical problems. This is the reason why it was successfully used only in discrete ordinate models where its integration is necessary only on a few directions [10].

Anhydrous samples (4 days in an oven at 80 °C, followed by 10 min in a silica gel desiccators at 20 °C) and samples equilibrated at an ambient humidity (65% RH) were investigated. Five replicates of each knitted samples were measured at 1.94 μm corresponding to the laser wavelength used in the photothermal experiment.

Actually, in the model presented in Section 1, the optical absorption coefficient and the scattering coefficient appear always multiplied by the thickness, meaning that the relevant parameters from global optical point of view are the dimensionless products: optical thickness ($K \cdot l$) and scattering thickness ($\sigma \cdot l$). Therefore the three identified values obtained from the least-squared minimization program were $K \cdot l$, $\sigma \cdot l$ and a. Then the corresponding optical absorption and scattering coefficients can be calculated for any value of the sample thickness. The precisions on the optical related coefficients are of 4%, 7% and 0.2 for optical absorption coefficient, scattering coefficient and geometrical factor respectively.

Fig. 6 shows the values of the optical thickness for the two cases: anhydrous samples (open symbols) and samples at ambient relative humidity. The optical thickness for a certain yarn number is decreasing with the absorbed stitch length which is normal, since the larger this value, the less dense the fabric. Actually, for a dry sample, the absorption coefficient K and optical thickness $K \cdot l$ are proportional to the density and the mass per area respectively. The absorption coefficient is increasing strongly with the water content, since it is measured at a wavelength corresponding to an absorption band of water. In average there is a 60% increase of the absorption coefficient K for a 6% increase of the water content W (value for cotton at 65% RH).

In Fig. 7 is presented the scattering thickness σl for the 9 types of samples. At a given humidity, the scattering thickness is decreasing with the absorbed stitch length. The scattering coefficient is increasing with the density of the fabric and decreasing with the water content, in average about 7% for a 6% increase of the water content.

The positive value of the asymmetry factor a confirm a forward tendency of the phase function (Fig. 8), increasing with the absorbed stitch length. We observe that the influence of the water content on this parameter is smaller than the experimental errors.

3.2. Thermal parameters

The PPE prototype and experimental set-up are presented elsewhere [2,11]. Here are given only a few details. A 200 μm thick and 20 mm diameter PZT ceramic provided with high reflectance gold electrodes, was used as a

pyroelectric sensor. The textile sample is a disk clamped between two PVC rings generating a constant and reproducible pressure. The relatively small but nevertheless necessary generated tension ensures the flatness of the sample. The reproducibility has been confirmed by a series of measurements done on different samples coming from the same textile specimen (standard deviation of 5% on the amplitude and 1deg on the phase).The experimental errors integrate the eventual differences in the sample positioning and heterogeneities of the sample. The experimental errors on the electronic signal are within the errors announced above.

The PPE signal data were measured by a Stanford Research SR850 lock-in amplifier. The diode laser (Applied Optronics Corp.) was electronically modulated by the internal generator of the lock-in. Its average power was about 1 mW. The experiment was computer controlled via an RS 232 interface and a LabView 6.01 program. The experimental data were processed and inversed by a Mathematica 3.0 program based on a Levenberg–Marquart algorithm. The unknown parameters which are identified are the volume specific heat, the thermal conductivity and the air gap thickness. The other thermal parameters (thermal diffusivity, thermal effusivity and thermal resistance) are calculated.

The diode laser is fixed on a temperature controlled Peltier element. The temperature control unit serves to stabilize the output energy of the diode laser and can also be used for a small range tuning of the wavelength. The diode laser is connected to an optical fiber and then to a collimator. The wavelength was 1.94 ± 0.01 µm and the average power of the incoming collimated beam was about 1 mW with a spot diameter of about 5 mm. The PPE signal (amplitude and phase) was measured in the range 0.01–100 Hz, 10 points per decade.

The thickness measurement for a textile sample is delicate task since it has to be done at a certain pressure applied to the sample. We have chosen to work with the two values of thickness given by the international standard method [18] because we wanted our results to be comparable to the ones obtained in the textile industry.

The air gap thickness parameter integrate not only the equivalent air thickness between the sensor and the sample but also the heterogeneities of the interface air/sample.

In Fig. 9 is presented the volume specific heat for the two values of thickness, for the dry materials. The two curves differ only by a factor depending on the ratio of the calculated densities. In other words, the specific heat: $c = C/\rho$ is the same for the two identifications within the errors of calculated values.

We observe in Fig. 10 that the thermal conductivity is larger when we consider a larger value of the thickness. (*N.B.* The "real" thickness is the same.) The thermal resistance over the unit area R_{th} defined as the ratio between the sample thickness and its thermal conductivity is shown in Fig. 11 (open symbols for dry materials). We observe that the thermal resistance is the same within the errors for the two identifications, meaning that we can apparently obtain a

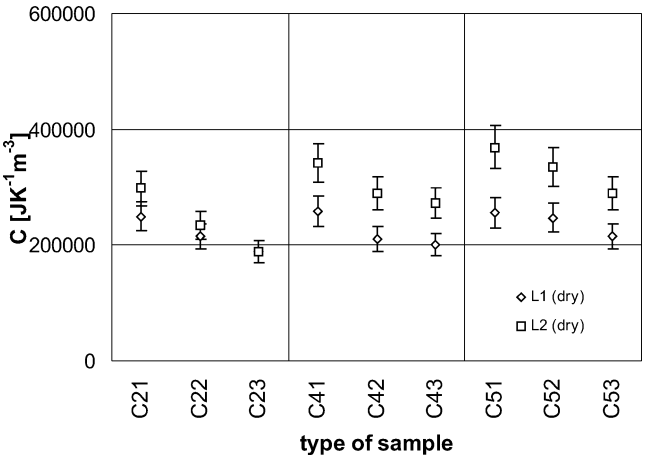

Fig. 9. The volume specific heat of the dry cotton samples calculated with two values of the sample's thickness.

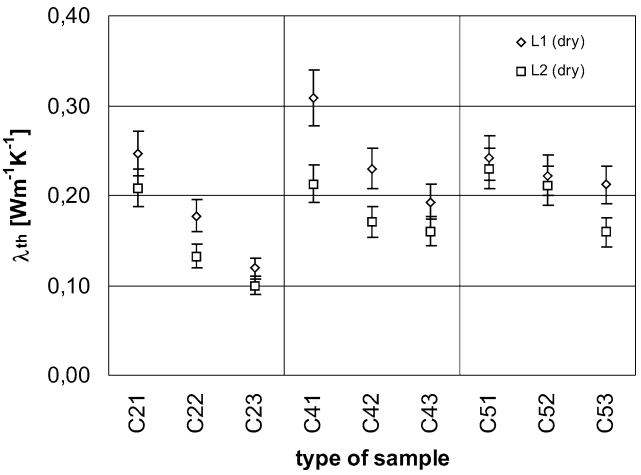

Fig. 10. Same as Fig. 9 for the thermal conductivity.

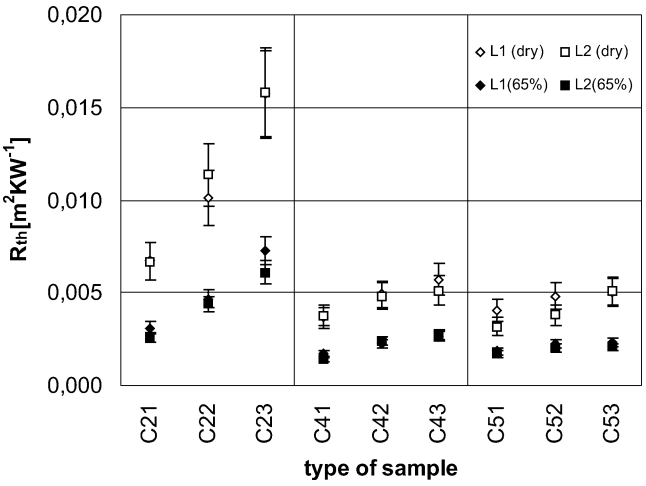

Fig. 11. The thermal resistance for dry (open symbols) and ambient humidity (filled symbols) cotton samples.

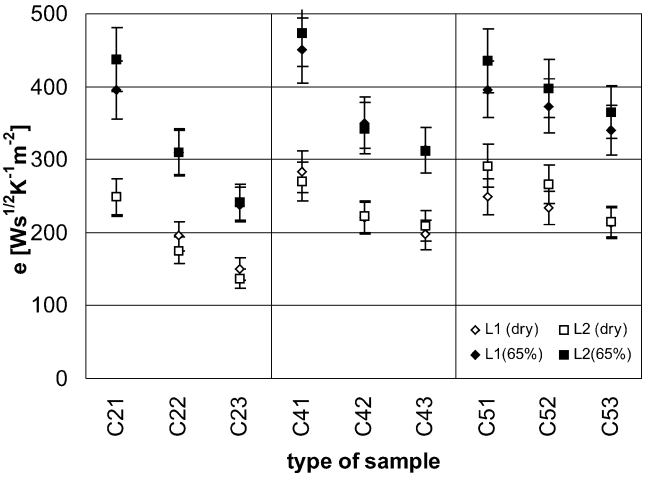

Fig. 12. Same as Fig. 11 for the thermal effusivity.

larger conductivity when considering a larger value for the thickness but the result in terms of thermal insulation is the same. In Fig. 11 are also presented the values of the thermal resistance for the samples at ambient humidity. The values are smaller when the fabrics contain water, as expected.

The calculated thermal effusivity $e = (C\lambda_{\text{th}})^{1/2}$ is also insensitive to the value of the thickness (Fig. 12). This could be explained by the fact that the effusivity is a parameter related to the interface and it should not depend on the thickness of the sample behind this interface. This observation is important in the comfort estimation. The effusivity of a humid material is larger that the one of a dry one, from where the "warm-cool feeling". The thermal effusivity enters into the handle estimation of a tissue by the method of Kawabata [19] as being the only thermal parameter taken into account among some other ten mechanical parameters.

4. Conclusion

The PPE model in a noncontact configuration was modified in order to take into account the scattering effect. A four-flux model was developed initially for optical parameter identification of textile from experimental data obtained from a spectrophotometer equipped with an integrating sphere. Then, the four-flux model was adapted for the PPE configuration. This allowed for the thermal properties characterization of textile samples function of structure and water content.

The main advantage of our laboratory prototype relies on its reproducible and pressure independent results. But the method is not a true noncontact one since the distance between sensor and sample has to be controlled in the submillimetre range. This is the reason why the PPE method will always remain at laboratory device level.

Our approach contained some obviously simplified assumptions: the fact that the sample is considered thermally homogeneous and the optical parameters (absorption and scattering coefficients) are global values characterizing the sample as a whole. These assumptions are however sufficient since in practice, the comfort of a fabric with respect to water is given by the "warm-cool feeling" given by the thermal effusivity and the insulation properties. The latter is well characterised by the thermal resistance and its dependence on the water content.

A more detailed discussion on the inversion method, on the possibility of detecting both optical and thermal parameters of textile samples from only PPE measurement is given on the second article from this back-to-back series [17].

Appendix A. Modeling of the radiative properties of textile samples

A material is scattering if it consists of heterogeneous zones having different refractive index values. We are going to characterize an equivalent, homogeneous material, having from macroscopic point of view the same radiative properties. The radiative transfer equation in such an equivalent homogeneous material is given by the general form [12,13]:

$$\frac{\mathrm{d}L_\lambda(s,\Omega)}{\mathrm{d}s} = -(K_\lambda+\sigma_\lambda)L_\lambda(s,\Omega) + K_\lambda L_\lambda^0\big[T(s)\big] + \frac{\sigma_\lambda}{4\pi}\int_{4\pi} p_\lambda\big(s,\Omega',\Omega\big)L_\lambda\big(s,\Omega'\big)\,\mathrm{d}\Omega' \quad \text{(A.1)}$$

at any point of abscissa s, in the direction Ω characterized by the angles θ et φ, where K_λ and σ_λ are respectively the absorption and scattering coefficient, and p_λ the phase function.

Four-flux approach

From now on the monochromatic index will be omitted. The fundamental hypothesis of the four flux approach is to divide the intensity inside the material into four components: two directional collimated components (I^+ and I^-) obtained from the incident flux upon reflections and transmissions on the two interfaces of the sample and two isotropic components (L^+ and L^-) on each half-space [9, 10].

In one-dimensional geometry of abscissa x, with θ_p and θ_m the angles of I^+ and I^- of directions Ω_p and Ω_m inside the sample, Eq. (A.1) becomes:

For the directions with $\cos\theta > 0$:

$$L(x,\Omega) = I^+(x)\delta(\Omega-\Omega_p) + L^+(x) \quad \text{(A.2a)}$$

For the directions with $\cos\theta < 0$:

$$L(x,\Omega) = I^-(x)\delta(\Omega-\Omega_m) + L^-(x) \quad \text{(A.2b)}$$

The Dirac function is defined by:

$$\delta(\Omega-\Omega_0) \equiv \delta(\cos\theta-\cos\theta_0)\delta(\varphi-\varphi_0) \quad \text{(A.3)}$$

By introducing into the transfer equation the values taken by $L(x,\Omega)$ in each of the two half-spaces we obtain four

partially coupled differential equations. On the particular directions $\theta = \theta_p$ and $\theta = \theta_m$, the transfer equation contains only the collimated fluxes. At normal incidence, ($\theta_p = 0°$ and $\theta_m = 180°$) the transfer equations for the collimated beams are:

$$\begin{aligned}&\frac{\mathrm{d}I^+(x)}{\mathrm{d}x} + (K+\sigma)I^+(x) = 0\\ &\frac{\mathrm{d}I^-(x)}{\mathrm{d}x} + (K+\sigma)I^-(x) = 0\end{aligned} \tag{A.4}$$

having the following solutions:

$$\begin{aligned}&I^+(x) = I_p \exp\bigl[-(K+\sigma)x\bigr] \quad \text{and}\\ &I^-(x) = I_m \exp\bigl[(K+\sigma)x\bigr]\end{aligned} \tag{A.5}$$

The integration constants I_p and I_m are calculated using the boundary conditions and depend on the transmission and the reflection coefficients of the two surfaces (τ_0, ρ_0) and (τ_l, ρ_l) and on the incident flux I_0:

$$I^+(0) = \tau_0 I_0 + \rho_0 I^-(0) \quad \text{and} \quad I^-(l) = \rho_1 I^+(l) \tag{A.6a}$$

If the specular reflections at the two surfaces are neglected as it is the case for fibrous samples:

$$I^+(0) = I_0 \quad \text{and} \quad I^-(l) = 0 \tag{A.6b}$$

we obtain $I_p = I_0$ et $I_m = 0$, and the collimated flux I^- is zero, reducing the number of fluxes to three. For the directions of positive $\cos\theta$ and for $\theta \neq \theta_p$, Eq. (A.2a) becomes:

$$\begin{aligned}&\cos\theta\frac{\mathrm{d}L^+(x)}{\mathrm{d}x} + (K+\sigma)L^+(x)\\ &\quad = KL^0\bigl[T(x)\bigr] + \frac{\sigma}{4\pi}I^+(x)p(\Omega_p,\Omega)\\ &\qquad + \frac{\sigma}{4\pi}L^+(x)\int\limits_{\cos\theta>0} p(\Omega',\Omega)\,\mathrm{d}\Omega'\\ &\qquad + \frac{\sigma}{4\pi}I^-(x)p(\Omega_m,\Omega)\\ &\qquad + \frac{\sigma}{4\pi}L^-(x)\int\limits_{\cos\theta<0} p(\Omega',\Omega)\,\mathrm{d}\Omega'\end{aligned} \tag{A.7a}$$

For the directions of negative $\cos\theta$ and for $\theta \neq \theta_m$, Eq. (A.2b) becomes:

$$\begin{aligned}&\cos\theta\frac{\mathrm{d}L^-(x)}{\mathrm{d}x} + (K+\sigma)L^-(x)\\ &\quad = KL^0\bigl[T(x)\bigr] + \frac{\sigma}{4\pi}I^+(x)p(\Omega_p,\Omega)\\ &\qquad + \frac{\sigma}{4\pi}L^+(x)\int\limits_{\cos\theta>0} p(\Omega',\Omega)\,\mathrm{d}\Omega'\\ &\qquad + \frac{\sigma}{4\pi}I^-(x)p(\Omega_m,\Omega)\\ &\qquad + \frac{\sigma}{4\pi}L^-(x)\int\limits_{\cos\theta<0} p(\Omega',\Omega)\,\mathrm{d}\Omega'\end{aligned} \tag{A.7b}$$

By introducing into the transfer equation the values taken by the scattered fluxes $L(x,\Omega)$ in each of the two half-spaces we obtain four coupled equations. We integrate each of the equation over its validity domain. This operation determine the appearance of some integrals of the phase function:

$$\begin{aligned}\sigma_t &= \frac{\sigma}{8\pi^2}\int\limits_{\cos\theta>0}\int\limits_{\cos\theta'>0} p(\Omega',\Omega)\,\mathrm{d}\Omega'\,\mathrm{d}\Omega\\ &= \frac{\sigma}{8\pi^2}\int\limits_{\cos\theta<0}\int\limits_{\cos\theta'<0} p(\Omega',\Omega)\,\mathrm{d}\Omega'\,\mathrm{d}\Omega\\ \sigma_r &= \frac{\sigma}{8\pi^2}\int\limits_{\cos\theta>0}\int\limits_{\cos\theta'<0} p(\Omega',\Omega)\,\mathrm{d}\Omega'\,\mathrm{d}\Omega\\ &= \frac{\sigma}{8\pi^2}\int\limits_{\cos\theta<0}\int\limits_{\cos\theta'>0} p(\Omega',\Omega)\,\mathrm{d}\Omega'\,\mathrm{d}\Omega\end{aligned} \tag{A.8}$$

The coefficients σ_t and σ_r are respectively the forward ($\cos\theta$ and $\cos\theta'$ having the same sign) and backward scattering ($\cos\theta$ and $\cos\theta'$ having opposite signs) coefficients. The integrals on a half-space relative at an incident direction give the following coefficients:

$$\begin{aligned}\sigma_T &= \frac{\sigma}{4\pi}\int\limits_{\cos\theta>0} p(\Omega_p,\Omega)\,\mathrm{d}\Omega = \frac{\sigma}{4\pi}\int\limits_{\cos\theta<0} p(\Omega_m,\Omega)\,\mathrm{d}\Omega\\ \sigma_R &= \frac{\sigma}{4\pi}\int\limits_{\cos\theta<0} p(\Omega_p,\Omega)\,\mathrm{d}\Omega = \frac{\sigma}{4\pi}\int\limits_{\cos\theta>0} p(\Omega_m,\Omega)\,\mathrm{d}\Omega\end{aligned} \tag{A.9}$$

Since the non-normalized phase function integrated over the entire space is equal to 4π, the sum of the partial scattering coefficients is equal to the global scattering coefficient of the material:

$$\sigma_t + \sigma_r = \sigma_T + \sigma_R = \sigma \tag{A.10}$$

After integration of the transfer equation, and in the case where the emission of the medium can be neglected (cold medium approximation) we are looking for solutions of the form:

$$\begin{aligned}&L^+(x) = a^+e^{-\gamma x} + b^+e^{\gamma x} + c^+e^{-\beta x} + d^+e^{\beta x}\\ &L^-(x) = a^-e^{-\gamma x} + b^-e^{\gamma x} + c^-e^{-\beta x} + d^-e^{\beta x}\end{aligned} \tag{A.11}$$

where $\beta = K + \sigma$ is the extinction coefficient and $\gamma = 2\sqrt{K(K+2\sigma_r)}$.

In the case of textiles, the directional flux I^- is equal to zero, meaning that d^+ and d^- are also equal to zero. The other constants: a^+, a^-, b^+, b^- are calculated from the boundary conditions at $x = 0$ and $x = l$. By neglecting the reflections at the interfaces, we obtain:

$$L^+(0) = L^-(l) = 0 \tag{A.12}$$

Calculus of directional–hemispherical properties

Our objective is the determination of the absorption and scattering coefficients and of the phase function of textile samples from experimental data obtained with a spectrophotometer equipped with an integrating sphere.

Therefore, we have to relate the directional–hemispherical properties to the absorption–scattering coefficients.

For normal incidence, the directional transmittance is given by:

$$\tau' = \frac{I^+(l)}{I_0} = \frac{I_0 e^{-\beta l}}{I_0} = e^{-\beta l} \tag{A.13}$$

The hemispherical transmittance $\tau'^{\cap}$ is obtained from:

$$\tau'^{\cap} = \frac{\pi L^+(l)}{I_0} = \frac{\pi (a^+ e^{-\gamma l} + b^+ e^{\gamma l} + c^+ e^{-\beta l})}{I_0} \tag{A.14}$$

The hemispherical reflectance $\rho'^{\cap}$ is given by:

$$\rho'^{\cap} = \frac{\pi L^-(0)}{I_0} = \frac{\pi (a^- + b^- + c^-)}{I_0} \tag{A.15}$$

Phase function representation

Three macroscopic values of radiative parameters are accessible with a spectrophotometer provided with an integrating sphere: the directional transmittance and the hemispherical reflectance and transmittance. Therefore, the maximum number of parameters that can be obtained experimentally is three. For this reason we have chosen for phase function representation, only functions depending on one parameter at most.

For the case of isotropic scattering: $p(\theta_0) = 1$, the scattering coefficients defined by Eqs. (A.8) and (A.9):

$$\sigma_t = \sigma_r = \sigma_T = \sigma_R = \frac{\sigma}{2} \tag{A.16}$$

If the scattering is supposed linearly anisotropic, the phase function is:

$$p(\theta_0) = 1 + a\cos\theta_0 \tag{A.17}$$

This type of function allows the representation of slightly anisotropic scattering. The scattering coefficients are:

$$\begin{aligned} &\sigma_t = \frac{\sigma}{2}\left(1 + \frac{a}{4}\right) \quad \text{and} \quad \sigma_r = \frac{\sigma}{2}\left(1 - \frac{a}{4}\right) \\ &\sigma_T = \frac{\sigma}{2}\left(1 + \frac{a}{2}\right) \quad \text{and} \quad \sigma_R = \frac{\sigma}{2}\left(1 - \frac{a}{2}\right) \end{aligned} \tag{A.18}$$

The Henyey–Greenstein function is adapted for modelling scattering processes strongly forward oriented:

$$p(\theta_0) = \frac{1 - g^2}{(1 + g^2 - 2g\cos\theta_0)^{3/2}} \tag{A.19}$$

This function depends on one parameter but it can be integrated only numerically. This is the reason why it was successfully used only in discrete ordinate models where its integration is necessary only on a few directions [10].

References

[1] M. Chirtoc, D. Dadarlat, D. Bicanic, J.-S. Antoniow, M. Egee, in: A. Mandelis, P. Hess (Eds.), Progress in Photothermal and Photoacoustic Science and Technology; Vol. III: Life and Earth Sciences, in: PM, Vol. 41, SPIE Optical Eng. Press, Bellingham, WA, 1997, pp. 185–251.

[2] A. Frandas, T. Duvaut, D. Paris, Inverse analysis of water profile in starch by non contact photopyroelectric method, Appl. Phys. B 70 (2000) 77–84.

[3] R. Hüttner, T. Bahners, E. Schollmeyer, A. Weber, W. Backer, B. Bein, J. Pelzl, Detection of thermal waves by infrared radiometry as a tool for on-line characterization of thermal process in polymeric coatings and textiles, High Temp. High Press. 29 (1997) 379–384.

[4] T. Hüttner, E. Bahners, A. Schollmeyer, W. Weber, B. Backer, B. Bein, J. Pelzl, Modulated photothermal infrared radiometry as a tool for on-line characterization of polymeric coatings in textile processes, Progr. Natural Sci. Suppl. 6 (1996) S735–S738.

[5] I. Hess, J. Dolezal, New method and equipment for measuring thermal properties of textiles, Text. Mach. Soc. Japan 42 (1989) 71–75.

[6] M.J. Pac, Les surfaces textiles aux échelles micro, méso et macroscopiques : propriétés thermiques et tribologiques, Ph.D. Thesis, University of "Haute Alsace", Mulhouse, Fr., 2001.

[7] International Standard: ISO 11092, 1993.

[8] V.P. Nicolau, M. Raynaud, J.F. Sacadura, Spectral radiative properties identification of fiber insulating materials, Internat. J. Heat Mass Transfer 37 (7) (1994) 311–324.

[9] C. Bissieux, J.-F. Henry, P. Egée, Caractérisation radiative de matériaux semi-transparents diffusants à l'aide d'un modèle à quatre flux, Rev. Gen. Therm. 392 (1994) 470–478.

[10] J.-F. Henry, C. Bissieux, S. Marquié, Y. Gillet, One-dimensional modelling and parameter estimation in scattering media, High Temp. High Press. 29 (1997) 159–164.

[11] T. Duvaut, A. Limare, J.-M. Bachmann, Photothermal device for water dynamics measurement and thermophysical characterization: Application on textile sample, Rev. Sci. Instrum. 73 (2002) 1299–1303.

[12] R. Siegel, J.R. Howell, Thermal Heat Transfer, Hemisphere/McGraw-Hill, New York, 1992.

[13] M.N. Ozisik, Radiative Transfer and Interaction with Conduction and Convection, Wiley, New York, 1973.

[14] K. Levenberg, A method for the solution of certain problems in least-squares, Quant. Appl. Math. 2 (1944) 164–168.

[15] D.W. Marquardt, An algorithm for least squares estimation of non-linear parameters, J. Soc. Indust. Appl. Math. 2 (1963) 431–441.

[16] D. Paris, Etude de la migration d'humidité dans des biopolymers à base d'amidon par méthode photopyroélectrique, Ph.D. Thesis, University of Reims, Fr., 1998.

[17] A. Limare, T. Duvaut, J.-M. Bachmann, Photopyroelectrical measurement of the thermal properties of knitted textile samples, Influence of composition, structural parameters and water content, Internat. J. Therm. Sci., submitted together with this article.

[18] International Standard: ISO 9863-2, 1996.

[19] S. Kawabata, Y. Akagi, The standardization and analysis of hand evaluation, J. Text. Mach. Soc. Japan 23 (1977) 51–55.